

START-UP OF FEL OSCILLATOR FROM SHOT NOISE

V. Kumar*, S. Krishnagopal, RRCAT, Indore, M.P. 452013, India
W.M. Fawley, LBNL, Berkeley, CA 94720, USA

Abstract

In free-electron laser (FEL) oscillators, as in self-amplified spontaneous emission (SASE) FELs, the build-up of cavity power starts from shot noise resulting from the discreteness of electronic charge. It is important to do the start-up analysis for the build-up of cavity power in order to fix the macropulse width from the electron accelerator such that the system reaches saturation. In this paper, we use the time-dependent simulation code GINGER[1] to perform this analysis. We present results of this analysis for the parameters of the Compact Ultrafast TeraHertz FEL (CUTE-FEL) [2] being built at RRCAT.

INTRODUCTION

In an FEL oscillator driven by a pulsed radio-frequency linear accelerator, the growth of radiation starts from the noise present in the electron microbunches and gets further amplified in multiple passes, over the duration of the electron macropulse. The radiation power in the FEL cavity must saturate early enough such that one gets a temporally clean, usable radiation pulse for a significant portion of the electron macropulse. In this context, it is important to perform the start-up analysis while designing an FEL oscillator, as has been emphasized by many authors [3-9].

For typical oscillator parameters, quantum effects can be neglected [5,8] and the build-up of radiation starts from classical shot noise. Including the shot noise in the analysis of the interaction of an electron bunch with the radiation field in an FEL oscillator poses several challenges. First, the discreteness of charge has to be taken into account correctly, since the shot noise essentially results from this. Second, one has to include the broad bandwidth of radiation while studying the evolution of shot noise. This typically necessitates the use of time-dependent codes.

There have been earlier attempts to address these issues for FEL oscillators. Sprangle *et al.* [3,4] have studied the start-up process in FEL oscillators analytically, including the discrete nature of electrons, multiple radiation frequencies and finite pulse structure. The analysis, however, ignores the important non-linear effects and warm beam effects, and the three-dimensional effects are included only heuristically in terms of filling factors. Kuruma *et al.* [6] have studied the problem numerically using a one-dimensional, multi-frequency code where they have simulated the evolution of shot noise. Here also, three-dimensional effects have been ignored. In this paper, we simulate the start-up from shot noise of an FEL oscillator using the polychromatic FEL code GINGER [1] which

takes three-dimensional effects into account. In the next section, we discuss the details of simulations that we have performed for CUTE-FEL being developed at RRCAT. The results are discussed in the following section and finally we present some conclusions.

NUMERICAL SIMULATION

For simulating the start-up from shot noise, we have used the FEL code GINGER [1], a multidimensional [full 3D for macroparticle and 2D ($r-z$) for radiation], time-dependent code to simulate FEL interaction in single-pass amplifier as well as oscillator configurations. GINGER utilizes the KMR [10] wiggle-period-averaged electron-radiation interaction equations and the slowly-varying envelope approximation (SVEA) in both time and space for radiation propagation. For propagation outside the undulator for oscillator problems, the code uses a Huygens integral method. Shot noise is modeled by giving a controlled amount of randomness to the initial longitudinal phases of macroparticles; the algorithm [11] generates the statistically-correct shot noise at the fundamental as well as at harmonics.

The design parameters of CUTE-FEL are given in Table 1. For the simulations reported here, we have used $\gamma = 20.53$, where γ is the electron energy in unit of its rest mass energy. We had earlier done the time-independent simulation of CUTE-FEL using the code TDAOSC [12] which is an oscillator version of the code TDA [13]. For the parameters mentioned in Table 1, we had obtained a single pass, small signal gain (\equiv ssg) of 88%, saturated cavity power of 9 MW and hole out-coupled power of 0.65 MW. TDAOSC models the hole outcoupling in the mirror and the optimum hole radius was found to be 2 mm. The resonator parameters were also optimized using TDAOSC. The round trip radiation loss was calculated to be 15%, of which 7.5% was due to hole outcoupling, 2.5% due to mirror reflectivity, and 5% due to diffraction loss. Because GINGER does not model hole out-coupling, we instead put a total of 10% loss mirror reflectivity. This value includes a 7.5% loss from hole out-coupling and 2.5% from the actual mirror reflectivity. Note that GINGER does include diffraction and refraction effects.

We first performed time-independent simulation using GINGER in order to verify our old results and obtain a single pass ssg of 90% and saturated cavity power of 8.3 MW. Assuming 7.5% out-coupling, the out-coupled power becomes 0.62 MW. These numbers agree quite well with earlier results of Ref. 12. We then proceeded with time-dependent oscillator simulations adopting a Gaussian longitudinal electron beam profile with a rms width of 4 ps and peak current of 20 A ($Q = 0.2$ nC). The longitudinal slice

* vinit@cat.ernet.in

Table 1: CUTE-FEL design parameters

Electron beam energy (E)	10 MeV
Peak beam current (I)	20 A
RMS energy spread (σ_γ/γ)	0.5%
RMS normalised emittance	30 π mm-mrad
RMS pulse width (σ_z)	1.2 mm
Micropulse rep. rate	36.62 MHz.
RMS e-beam size (σ_x, σ_y)	0.65 mm, 2.00 mm
Electron macropulse width	8 μ s
Undulator period (λ_u)	50 mm
Peak und. parameter (K)	0.8
Undulator length ($N_u \lambda_u$)	2.5 m
Undulator gap	35 mm
Beam pipe diameter	28 mm (ID)
Radiation wavelength (λ_R)	80 μ m
Optical cavity length	4.1 m
Location of down. mirror	65 cm from und. exit
Location of up. mirror	95 cm from und. entr.
Mirror radii of curvature	2.25 m (d), 2.5 m (u)
Mirror reflectivity (power)	99%
Hole radius in down. mirror	2 mm

spacing was two radiation wavelengths. In the next section, we discuss the results of the time-dependent simulation.

RESULTS

We have studied the variation in the single pass ssg with cavity detuning ΔL_c . As is well known, there is no gain at zero cavity detuning and one must reduce the cavity length slightly in order to get positive gain [14]. Fig. 1 shows the net round trip gain as a function of cavity detuning from the synchronized cavity length 4.1 m. We find that maximum gain occurs for $\Delta L_c \approx 80 \mu\text{m}$ with a net round trip gain of 21%, equivalent to gain in the undulator of 36%. In the time-independent simulation, where the pulse structure and the slippage were ignored, the maximum ssg was 90%. One can also use the following analytical formula of Dattoli et al. [15] to predict the effects of finite pulse width:

$$g = \frac{g_0}{1 + \frac{1}{3}\mu_c}, \quad (1)$$

where g and g_0 are the ssg with and without finite pulse effect respectively, $\mu_c = N_u \lambda_R / \sigma_z$, N_u is the number of undulator periods, λ_R is the radiation wavelength and σ_z is the rms electron pulse length. Using the above formula, the ssg after including the time-dependent effect is obtained to be 42%. This agrees well with GINGER calculation.

Figure 2 displays the evolution of power spectrum where one sees that the initially broad band noise evolves to a sharper spectrum - unlike in the case of SASE, where the spectrum remains noisy. This occurs both from detuning and slippage effects and because the cavity preferentially filters out modes other than the fundamental cavity mode.

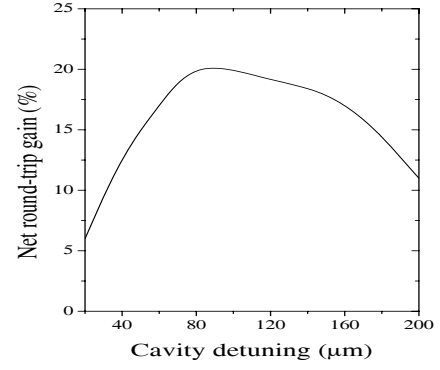


Figure 1: Net round-trip gain as a function of cavity detuning.

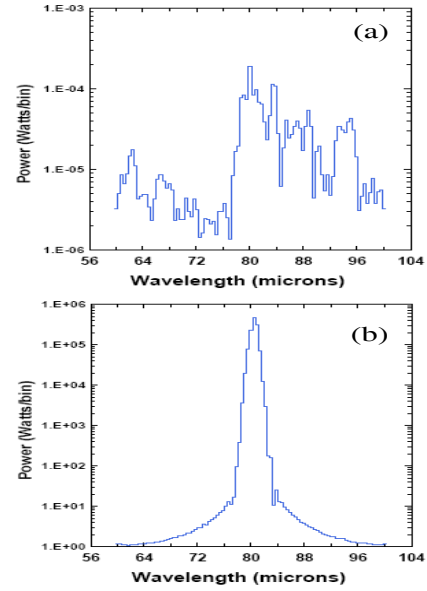


Figure 2: Power spectrum of the output signal after (a) first pass, and after (b) saturation.

Figure 3 shows the evolution of cavity power from shot noise for $\Delta L_c = 80 \mu\text{m}$. The cavity power saturates in around 135 passes. Since round trip time in this cavity is 27.3 ns, this means the start-up time is around 3.7 μs . It is interesting to compare the start-up time in FEL oscillator with saturation length in a SASE FEL. Here, the net round trip gain is 21% which means that power gets e-folded in around 5.25 passes. Hence, 135 passes is around 26 gain lengths. This is similar to growth of power in SASE FELs where it typically takes 20-30 power gain lengths for saturation [16]. Fig. 4 shows the variation in start-up time with ΔL_c . We have verified that at other detuning values the number of passes required for saturation is also equivalent to around 25 power gain lengths.

The variation of total energy in the out-coupled micropulse at saturation as a function of ΔL_c is shown in

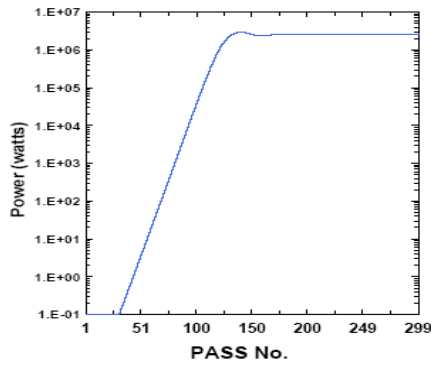


Figure 3: Average cavity power as a function of pass number. The power is averaged over the electron beam duration of 24 ps.

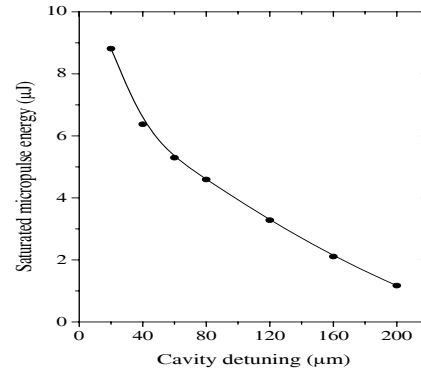


Figure 5: Variation of micropulse energy in the out-coupled pulse as a function of cavity detuning.

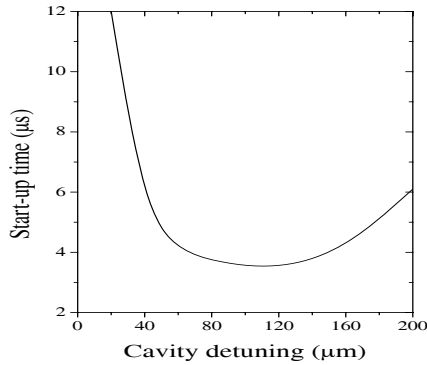


Figure 4: The variation of start-up time with cavity detuning.

Fig. 5. We find that as ΔL_c increases, the micropulse energy decreases. At lower detuning, the micropulse energy at saturation is large, but since gain is small, the start-up time will also be large. As is well known, at higher detuning where the small signal gain may be larger, the saturated power is smaller [14]. The 8- μ s electron macropulse width for RRCAT FEL corresponds to 300 passes. At lower cavity detuning values, it may then be difficult for the FEL to saturate. We therefore plan to operate around a cavity detuning of 80 μ m.

CONCLUSIONS

We have performed multidimensional, time-dependent simulations of start-up of the CUTE-FEL oscillator from shot noise including the effects of detuning, and outcoupling. We determined the start-up time for the design parameters is around 3.7 μ s. Furthermore, the number of passes required for the FEL to saturate is equivalent to 25 gain lengths, similar to single pass, SASE FELs.

REFERENCES

- [1] W. Fawley, *A user Manual for GINGER and Its Post-Processor XPLOTGIN*, LBNL-49625-Rev. I ed., Lawrence Berkley National Laboratory (2004).
- [2] S. Krishnagopal et al., Proceedings of FEL conference (2006) 496.
- [3] P. Sprangle, C. M. Tang and I. Bernstein, Phys. Rev. Lett. 50 (1983) 1775.
- [4] P. Sprangle, C. M. Tang and I. Bernstein, Nucl. Instr. and Meth. A 237 (1985) 41.
- [5] S. Benson, J. M. J. Madey, Nucl. Instr. and Meth. A 237 (1985) 55.
- [6] W. B. Colson, Nucl. Instr. and Meth. A 296 (1990) 348.
- [7] S. Kuruma et al., Nucl. Instr. and Meth. A 331 (1993) 421.
- [8] W. S. Graves, Nucl. Instr. and Meth. A 393 (1997) 210.
- [9] Z. Dong et al., Nucl. Instr. and Meth. A 475 (2001) 187.
- [10] N.M. Kroll, P.L. Morton, and M.R. Rosenbluth, IEEE J. Quantum Elec. QE-17, (1981) 1436.
- [11] W.M. Fawley, PRST-AB 5 (2002) 070701.
- [12] S. Krishnagopal et al., Nucl. Instr. and Meth. A 318 (1992) 661.
- [13] T. M. Tran, J. S. Wurtele, Computer Phys. Commun. 54 (1989) 263.
- [14] D. Oepts, in: J. Chen et al. (Eds.), *Development and Application of Free Electron Lasers*, Beijing, China; Proceedings of the CCAST symposium (Gordon and Beach, 1997).
- [15] G. Dattoli et al., Opt. Commun. 35 (1980) 407.
- [16] K.-J. Kim, Nucl. Instr. and Meth. A 250 (1986) 396.